ARTICLE
Journal of Cellular Biochemistry 116:320–330 (2015)

Journal of Cellular Biochemistry

Transcriptional Regulation of the Human *TNFSF11* Gene in T Cells Via A Cell Type-Selective Set of Distal Enhancers

Kathleen A. Bishop,[1] Xiaohua Wang,[2] Heidi M. Coy,[1] Mark B. Meyer,[1] Jenny E. Gumperz,[2] and J. Wesley Pike[1]*

[1]*Department of Biochemistry, University of Wisconsin-Madison, Madison, Wisconsin 53706*

[2]*Department of Medical Microbiology and Immunology, University of Wisconsin-Madison, Madison, Wisconsin 53706*

ABSTRACT

In addition to osteoblast lineage cells, the TNF-like factor receptor activator of NF-κB ligand (RANKL) is expressed in both B and T cells and may play a role in bone resorption. Rankl gene (*Tnfsf11*) expression in mouse T cells is mediated through multiple distal elements marked by increased transcription factor occupancy, histone tail acetylation, and RNA polymerase II recruitment. Little is known, however, of the regulation of human *TNFSF11* in T cells. Accordingly, we examined the consequence of T cell activation on the expression of this factor both in Jurkat cells and in primary human T cells. We then explored the mechanism of this regulation by scanning over 400 kb of DNA surrounding the *TNFSF11* locus for regulatory enhancers using ChIP-chip analysis. Histone H3/H4 acetylation enrichment identified putative regulatory regions located between −170 and −220 kb upstream of the human *TNFSF11* TSS that we designated the human T cell control region (hTCCR). This region showed high sequence conservation with the mouse TCCR. Inhibition of MEK1/2 by U0126 resulted in decreased RANKL expression suggesting that stimulation through MEK1/2 was a prerequisite. ChIP-chip analysis also revealed that c-FOS was recruited to the hTCCR as well. Importantly, both the human *TNFSF11* D5a/b (RLD5a/b) enhancer and segments of the hTCCR mediated robust inducible reporter activity following TCR activation. Finally, SNPs implicated in diseases characterized by dysregulated BMD co-localized to the hTCCR region. We conclude that the hTCCR region contains a cell-selective set of enhancers that plays an integral role in the transcriptional regulation of the *TNFSF11* gene in human T cells. J. Cell. Biochem.116: 320–330, 2015.

KEY WORDS: ChIP-CHIP ANALYSIS; T CELL RANKL; DISTAL ENHANCERS; EPIGENETIC MARKS; C-FOS

Receptor Activator of NF-κB ligand (RANKL) is primarily produced as a membrane bound ligand and interacts with Receptor Activator of NF-κB (RANK) on target cells to modulate cell differentiation, activation, and survival [Anderson et al., 1997; Wong et al., 1997b; Fata et al., 2000; Loser et al., 2006; Leibbrandt and Penninger, 2008]. Most notably, RANKL expression in osteoblasts stimulates osteoclast precursor differentiation into functional osteoclasts thereby increasing levels of bone resorption [Suda et al., 1992; Lacey et al., 1998; Jimi et al., 1999; Teitelbaum, 2000]. T cell expression of RANKL, on the other hand, has been shown to promote immune function through dendritic cell survival and expansion of T regulatory cells [Wong et al., 1997a,b; Loser et al., 2006]. Increased expression of RANKL has been implicated in many disease states, including post-menopausal osteoporosis [Silverman, 2009], autoimmune disease [Nakashima et al., 2003], cancer metastases targeted to the bone [Burkiewicz et al., 2009], and

Abbreviations: RANKL, receptor activator of NF-κB ligand; RANK, receptor activator of NF-κB; ChIP-chip, chromatin immunoprecipitation linked to tiled microarrays; Chip-seq, ChIP linked to deep sequencing; VDR, vitamin D receptor; CREB, cyclic AMP enhancer binding protein; RUNX2, runt related transcription factor 2; STAT3, signal transducer and activator of transcription 3; H4ac, histone H4 acetylation; H3K9ac, histone H3 lysine 9 acetylation; RNA pol II, RNA polymerase II; TCCR, T cell control region; hTCCR, human TCCR; TSS, transcriptional start site; PBMC, peripheral blood mononuclear cells; PMA, phorbol-12-myristate-13-acetate; PI, PMA/ionomycin; TPB, total peripheral blood T cells; c-Fos, cellular fos transcription factor; AP-1, activator protein 1; NFAT, nuclear factors of activated T cells; SNP, single nucleotide polymorphism; 1, 25$(OH)_2D_3$, 1, 25-dihydroxyvitamin D_3; BAC, bacterial artificial chromosome.

Current address for K.A. Bishop is Maine Medical Center Research Institute, Scarborough, ME 04074.

Current address for X. Wang is Department of Cell Biology, Albert Einstein College of Medicine, 1300 Morris Park Ave, Bronx, NY 10461.

Disclosure statement: The authors state that they have nothing to disclose.

Grant sponsor: National Institute of Health; Grant number: DK-74993.

*Correspondence to: J. Wesley Pike, Department of Biochemistry, Hector F. Deluca Research Laboratories, University of Wisconsin-Madison, 433 Babcock Drive, Madison, WI 53706. E-mail: pike@biochem.wisc.edu

Manuscript Received: 1 September 2014; Manuscript Accepted: 5 September 2014

Accepted manuscript online in Wiley Online Library (wileyonlinelibrary.com): 11 September 2014

DOI 10.1002/jcb.24974 • © 2014 Wiley Periodicals, Inc.

other chronic inflammatory diseases associated with increased bone loss [Leibbrandt and Penninger, 2008]. Because of its developing role centered on treatments for bone resorptive diseases, RANKL has become a major pharmacological target for modulation of bone resorption. The molecular mechanisms driving cell type-specific regulation of *Tnfsf11* (the Rankl gene) in the mouse have been recently explored [Bishop et al., 2011], but little is known of the regulation of the human *TNFSF11* gene [Kim et al., 2006b; Nerenz et al., 2008].

Transcriptional regulation of mouse *Rankl* has been well studied in osteoblastic cells initially using ChIP-chip analysis but more recently using ChIP-seq methods [Meyer et al., 2014a; Pike and Meyer, 2014; Pike et al., 2014]. Transcription is controlled by a series of at least six distal enhancers located −16 to −88 kb upstream of the mouse *Tnfsf11* transcriptional start site (TSS) that variably recruit VDR, CREB, Runx2, and STAT3 transcription factors as well as others. These enhancers act in an unknown fashion together with the *Tnfsf11* proximal promoter to modulate RANKL expression. The majority of the transcriptional activity has been mapped to two regulatory sites located at −75 to −77 and −88 kb upstream of the *Tnfsf11* TSS termed the mRLD5a/b and mRLD6 enhancers [Fu et al., 2006; Kim et al., 2006b, 2007; Bishop et al., 2009]. These transcriptionally responsive enhancers are marked by elevated levels of histone H4 acetylation (H4ac), histone H3 Lys9 acetylation (H3K9ac), as well as both RNA polymerase II and selective transcription factor recruitment [Bishop et al., 2009]. Both elevated histone acetylation and specific RNA polymerase II recruitment have been observed at these active transcriptional regulatory regions [Kurdistani et al., 2004; Schubeler et al., 2004; Roh et al., 2005, 2007]. Using the aforementioned markers as potential signatures of enhancer function, we identified several putative *Tnfsf11* enhancers in mouse T cells that include the mRLD5a/b region and a set of more distant enhancers located approximately 120–160 kb upstream of the *Tnsfs11* TSS which we termed the T cell control region (TCCR) [Bishop et al., 2011]. These putative enhancers were marked by high levels of monomethylated histone H3K4; this property satisfies one of the specific features now known to represent a beacon that highlights an active enhancer [Ernst et al., 2011]. Interestingly, the set of enhancers within the TCCR were not active in osteoblasts and thus provided the first evidence of cell type-specific enhancer activity associated with the *Tnfsf11* gene.

While some insight into the cell type-specific transcriptional regulation of the mouse *Tnfsf11* gene has been assembled, little is known about regulation of the human *TNFSF11* gene. Conserved sequences for the six mouse osteoblast enhancers are found upstream of the human *TNFSF11* gene, but only the hRLD1 and the hRLD5 enhancers at −20 and −95 kb, respectively, have been shown to be transcriptionally active in response to $1,25(OH)_2D_3$ [Nerenz et al., 2008]. Others have shown that a more promoter proximal NF-κB binding element may play a role in the upregulation of *TNFSF11* gene expression upon T cell activation [Fionda et al., 2007]. Inhibition of calcineurin by cyclosporin A has been observed to abrogate T cell activation-induced *TNFSF11* expression, suggesting the involvement of the NFAT family of transcription factors in the transcriptional regulation of this human gene [Wong et al., 1997b; Wang et al., 2002]. In this report, we provide an in depth analysis of the human *TNFSF11* locus in T cells. We used ChIP-chip analysis to screen the human *TNFSF11* locus in T cells for elevated levels of histone H4/H3 acetylation. Primary peripheral blood, naïve, memory, and Jurkat T cells were shown to exhibit elevated histone acetylation in a common region 170–220 kb upstream of the *TNFSF11* TSS that shares high sequence homology with that of the mouse TCCR. C-FOS was recruited to this human TCCR (hTCCR) following activation and cloned hTCCR fragments displaced inducible reporter activity upon T cell stimulation. We conclude that the human TCCR (hTCCR) is comprised of at least three distinct enhancer regions that play a collective role in the induction of *TNFSF11* transcription following T cell activation.

MATERIALS AND METHODS

REAGENTS

General biochemicals were purchased from ThermoFisher Scientific (Waltham, MA) and Sigma–Aldrich (St. Louis, MO). Phorbol-12-myristate-13-acetate (P8139) and ionomycin (I0634) were purchased from Sigma–Aldrich. Anti-c-FOS (sc-7202) antibody was obtained from Santa Cruz Biotechnology, Inc. (Santa Cruz, CA). Anti-acetyl histone H4 antibody (06-866) and anti-acetyl histone H3 Lys9 (06-942) were purchased from Millipore (Billerica, MA). Anti-RNA polymerase II 8WG16 (MMS-126R) was purchased from Covance (Princeton, NJ), Go Taq Flexi DNA polymerase (M8296) was purchased from Promega (Madison, WI), RPMI 1640 (10-040-CV) was purchased from Fisher Scientific (Pittsburg, PA), U0126 (662005) was purchased from Calbiochem (San Diego, CA), and Ficoll–Paque was purchased from GE Life Sciences (Uppsala, Sweden). Pan T cell preparation micro-beads (130–091-156) and CD45RO microbeads (130-046-001) were purchased from Miltenyi Biotec (Bergisch Gladbach, Germany). T4 DNA Ligase (M0202L) and T4 DNA Polymerase (M0203L) were obtained from New England Biolabs (Ipswich, MA). Lipofectamine (18324-012), Plus Reagent (10964-012), and DNaseI (18068-015) were purchased from Invitrogen Corporation (Carlsbad, CA). High Capacity cDNA Reverse Transcription Kit (4368813) and Power SYBR Green PCR Master Mix (4347660) were purchased from Applied BioSystems (Foster City, CA). Cy3 (N46-1019-CJ1A) and Cy5 (N46-0110-BS2A) 9-mer wobble primers were purchased from TriLink (San Diego, CA). Fetal bovine serum (FBS, SH30088.03) and penicillin/streptomycin (SV30010) were obtained from Hyclone (Logan, UT). QIAquick PCR Purification Kits (28106) and RNeasy Plus Mini Kits (74134) were purchased from Qiagen (Valencia, CA). Faststart SYBR Green (04673522001) was purchased from Roche (Basel, Switzerland); and NimbleGen Hybridization Kits (05223474001) and NimbleGen Wash Buffer Kits (05223504001) were purchased from Roche NimbleGen, Inc. (Madison, WI).

CELL CULTURE AND ISOLATION OF PRIMARY T CELLS

Jurkat cells were cultured in RPMI 1640 (Fisher) with 10% FBS (heat inactivated), 10 mM Hepes, pH 7.4, 2.5 mM Glutamine, 100 U/ml penicillin, and 100 μg/ml streptomycin. Fresh human peripheral blood mononuclear cells (PBMCs) were isolated from peripheral blood from healthy donors using standard Ficoll–Paque protocol

(GE life science). Studies were approved by the University of Wisconsin Minimal Risk Institutional Review Board, and written informed consent was obtained from all blood donors in accordance with the Declaration of Helsinki. PBMCs were then labeled with Pan T cell purification micro-beads and total T cells were purified under the standard auto-MACs protocol. Naïve and memory T cells were then separated using CD45RO microbeads. The CD45RO+ T cells were referred to as the memory T cell population, while the CD45RO- T cells were referred to as the Naïve T cell population. Cells were maintained in RPMI medium supplemented with 10% FBS plus 2.5 mM glutamine and were used for activation assays within 4 h of purification.

IN VITRO AND EX VIVO T CELL ACTIVATION

PMA/Ionomycin (PI) activation was accomplished by treating cells with 500 ng/ml ionomycin and 10 ng/ml phorbol-12-myristate-13-acetate (PMA). Primary T cells were activated by plate-bound CD3 antibody (OKT3, 5 μg/ml) and anti-CD11a (clone HI111, 0.5 μg/ml, Biolegend, CA) for 4 h.

RNA ISOLATION AND ANALYSIS

RNA was isolated using two methods: (1) Total RNA was isolated from cells using Tri-Reagent followed by DNaseI treament; or (2) RNA was isolated using the RNeasy Plus Mini Kit where cells were disrupted by pipetting up and down, processed through the gDNA eliminator column, and total RNA was isolated according to the manufacture′s protocol. RNA was reverse transcribed using the High Capacity cDNA Reverse Transcription Kit. The resulting cDNA was then subjected to qPCR analysis.

QUANTITATIVE PCR ANALYSIS

Real-time PCR was performed on an Eppendorf Realplex/ABI StepOnePlus using Power SYBR Master Mix with standard cycling conditions. The Mastercycler® ep realplex software or StepOne Software was used for analysis. Standard curves were made by serial dilutions of PCR-amplified cDNA. Primers used in the RNA analyses include: human *RANKL* mRNA: 5′-CCCATAAAGTGAGTCTGTCC-3′ (forward), 5′-CAATACTTGGTGCTTCCTCC-3′ (reverse); human β-actin mRNA: 5′-CAA GAT CAT TGC TCC TCC TGA-3′ (forward), 5′-TGC TGG AAG GTG GAC AGC-3′ (reverse); human *IL-2* mRNA: 5′-CTCACCAGGATGCTCACATTT-3′ (forward) and 5′-TTCAGATCCCTT-TAGTTCCAGA-3′ (reverse); human *FOS* mRNA: 5′-GTTGTGAAGAC-CATGACAGGAG-3′ (forward) and 5′-CTCCGCTTGGAGTGTATCAGT-3′ (reverse).

CHROMATIN IMMUNOPRECIPITATION-MICROARRAY ANALYSIS

ChIP analysis was performed as previously described [Yamamoto et al., 2003; Kim et al., 2005, 2006b, 2007]. Immunoprecipitated DNA was blunt-ended by T4 DNA Polymerase, ligated to linkers with the sequence 5′-GAATTCAGATC-3′ and 5′-GCGGTGACCCGG-GAGATCTGAATTC-3′ using T4 DNA ligase, and amplified by ligation-mediated PCR with Go Taq Flexi using successive rounds of linear PCR amplification. PCR purification was performed with the QIAquick PCR Purification Kit. DNA samples were labeled with Cy3 or Cy5 9-mer wobble primers using Klenow fragment, the reaction stopped with the addition of EDTA, precipitated with NaCl and isopropanol, washed with 80% EtOH and resuspended in water. Cy3- and Cy5-labeled DNA samples were co-hybridized to a custom oligonucleotide microarray using a NimbleGen Hybridization Kit and a MAUI hybridization system. Microarrays were washed using NimbleGen Wash Buffer and scanned using an Axon 4000B scanner with GenepixPro version 4.1 software at the appropriate wavelengths. Custom oligonucleotide microarrays were synthesized by Roche–NimbleGen Systems (Madison, WI). The microarray oligonucleotide probes were 50- to 70-mer in length with 65–70 bp resolution and synthesized using a mask-less array system tiled from 300 kb upstream of the human *RANKL* TSS to 50 kb downstream of the final 3′ coding exon. This custom array contained additional tiled genes not considered in this study. DNA samples were obtained by immunoprecipitation with antibodies specific for c-FOS, acetylated histone H4 Lys5,8,12, and 16 (H4ac), acetylated histone H3 Lys9 (H3K9ac), RNA polymerase II (RNA polymerase II), and a control rabbit IgG. A series of co-hybridizations were used: (1) untreated versus input control; (2) PI or CD3/LFA-1-treated versus input control; and (3) PI or CD3/LFA-1-treated versus vehicle-treated samples. The aforementioned co-hybridizations were analyzed and presented as previously described [Kim et al., 2006b]. Nimblescan version 1.9.0.05 was used for statistical analysis. Peaks were called using a sliding window of 700 bp containing at least four out of eight probes statistically above background was deemed significant.

PLASMIDS

Construction of the pTK-human *RANKL* (hRL) -D1, -D2, -D3, -D4, -D5a, and -D5b reporter constructs prepared in the thymidine kinase luciferase vector (pTK-luc) was previously described [Kim et al., 2006b; Nerenz et al., 2008; Bishop et al., 2009]. Similar methods were used to prepare the pTK-hRLD6 (−134590 to −134590), -T1A (−178452 to −176516), -T1B (−180931 to −178534), -T2 (−196498 to −195052), and the -T3 (−220304 to −218565) reporter constructs using primers containing HindIII/BamHI/SalI restriction sites. Digested fragments were cloned into the corresponding sites within the pTK-luc vector.

REPORTER TRANSFECTIONS

For transient transfections in Jurkat cells, cells were grown to ∼500,000 cells/ml, washed with PBS, and 50,000 cells/well were transfected with 250 ng reporter construct and 200 ng RSV-βgal using Lipofectamine and PLUS Reagent in serum-free media in 24 well plates. After a 3 h incubation, cells were supplemented with RPMI 1640 containing 20% FBS to a final concentration of 10% FBS and treated with 500 ng/ml ionomycin and 10 ng/ml PMA or DMSO vehicle. Cells were harvested 20 h later for reporter assays using lysis buffer, and both luciferase and β-galactosidase activities were determined as previously described [Kim et al., 2006b, 2007].

STATISTICAL ANALYSES

Values were expressed as the mean ± standard error of the mean. All statistical calculations were performed using GraphPad PRISM version 4 statistical software package (GraphPad Software Inc., San Diego¸ CA) using nonparametric *t* tests. Activated samples were contrasted with vehicle-treated controls or other indicated samples.

RESULTS

HUMAN RANKL MRNA LEVELS INCREASE FOLLOWING T CELL ACTIVATION

TNFSF11 expression in human T cells is known to increase with T cell activation in both in vitro and primary T cell model systems [Dai et al., 2004; Kanamaru et al., 2004; Gendron et al., 2005]. In order to confirm these findings and establish a model to study the mechanisms governing *TNFSF11* expression in human T cells, we utilized both the Jurkat cell line and primary human T cells. Jurkat cells were treated with PMA/ionomycin (PI); total RNA was isolated at several time points from 0 to 24 h post-activation, and the relative levels of RANKL mRNA were quantified using qRT-PCR (Fig. 1a). RANKL mRNA expression was maximal 3–6 h following T cell activation and transcript levels remained elevated through 24 h post-activation.

In order to validate the Jurkat cell line as a model system and investigate activation-induced RANKL expression in primary human T cells, human total peripheral blood (TPB) T cells were isolated and activated using anti-CD3/LFA-1 antibodies. RNA was isolated at several time points between 0 and 72 h post-activation, and RANKL transcript levels were quantified. RANKL expression transiently increased in the TPB T cells with maximal expression 3–6 h following activation and decreased in a time-dependent manner through 72 h (Fig. 1b) in a fashion similar to what has been previously observed in mouse CD4+ T cells [Bishop et al., 2011]. The TPB T cell population contains many types of T cells, including both naïve and memory T cells. Previous work has suggested that RANKL expression in both of these T cell types increases upon activation, although memory T cells in the mouse are believed to express RANKL at higher basal levels than naïve T cells [Josien et al., 1999]. To confirm and extend these observations, naïve and memory T cells were isolated from peripheral blood and then activated. RANKL expression in both T cell types showed a similar time course of induction when compared to total peripheral blood T cells, suggesting that both cell types likely contribute to RANKL expression in vivo (Fig. 1b and c). While the transient induction of RANKL expression following T cell activation was similar between mouse and human T cells [Bishop et al., 2011], both human naïve and memory T cells showed similar RANKL levels prior to and following activation, highlighting a potential difference between human and mouse.

CHIP-CHIP ANALYSIS REVEALS THE PRESENCE OF A HUMAN T CELL CONTROL REGION (hTCCR) IN JURKAT CELLS

ChIP-chip analysis of H4ac, H3K9ac, and RNA polymerase II (RNA pol II) in mouse T cells aided in the identification of enhancer regions at the *Tnfsf11* locus in both mouse osteoblasts and T cells, most notably at a unique set of putative enhancers located approximately 120 kb upstream of the mouse *Tnfsf11* TSS in T cells [Bishop et al., 2009, 2011]. In order to determine if similar enhancers might also be involved in regulating transcription of the human *TNFSF11* gene, we used this approach to define regions of elevated H4ac, H3K9ac, and RNA pol II occupancy in human T cells. Jurkat cells were treated with PI or vehicle for 6 h and

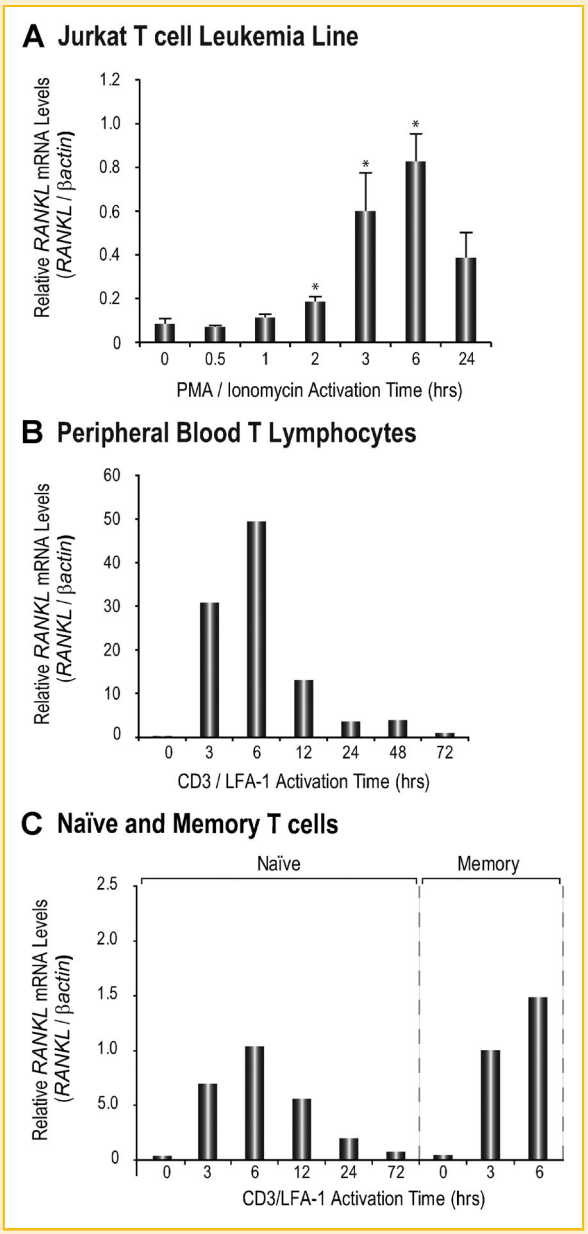

Fig. 1. Human *RANKL* mRNA levels are transiently induced with T cell activation. (A) Jurkat cells were treated with 500 ng/ml ionomycin and 10 ng/ml PMA or vehicle for up to 24 h, (B) human peripheral blood T cells, or (C) naïve/memory T cells were seeded in wells with or without plate bound CD3e and LFA-1 antibodies for up to 72 h. Total RNA was isolated at the indicated time points, reverse transcribed, and analyzed by qPCR using primers specific to *RANKL* and β-actin. *RANKL* transcript levels were normalized to β-actin. (A) Each value represents the average of three independent experiments ± SEM. $*P < 0.05$, is statistically significant using a non-parametric *t*-test when compared to control sample. $**P < 0.05$, is statistically significant using a non-parametric *t*-test when compared to both control samples and 6 h treatment samples. (B) Total peripheral blood T cells were isolated from a total of two donors as three different time points. Data shown is a representative of the three data sets. (C) Naïve/memory T cells were isolated from two donors at two time points. A representative data set is shown.

then evaluated by ChIP-chip analysis using antibodies to H4ac, H3K9ac, or RNA pol II. The resulting DNA fragments were amplified and co-hybridized with input samples to custom microarrays containing probes tiled over 300 kb upstream through 50 kb downstream of the human *TNFSF11* gene. The $\log_2$ ratio of fluorescence obtained from vehicle- or PI-treated samples precipitated with anti-H4ac (Fig. 2a), anti-H3K9ac (Fig. 2b), or anti-RNA polymerase II (RNA pol II) (Fig. 2c) are displayed in the indicated data tracks seen in the figure. Importantly, elevated levels of H4ac, H3K9ac and increased RNA pol II occupancy were found at sites between 170 and 220 kb upstream of the *TNFSF11* transcriptional start site (TSS); these features did not appear to be inducible by PI. Some enrichment of the H4ac mark, but not of H3K9ac or RNA pol II, was also evident at the RANKL enhancer regions termed hRLD3-hRLD5 as well, although these regions were not marked by either H3K9ac or recruitment of RNA pol II. We termed this intergenic region the hTCCR because it demonstrated not only high levels of sequence conservation when compared to the mouse TCCR (data not shown) [Bishop et al., 2011], but because there were similar histone markings and RNA pol II occupancy as well. Histone acetylation has been associated with regions containing a more open chromatin conformation allowing for the recruitment of transcription factors [Roh et al., 2005, 2007; Wang et al., 2008; Choi and Howe, 2009]. Thus, we conclude that the hTCCR may represent an important novel *TNFSF11* gene regulatory region in T cells.

CHIP-CHIP ANALYSIS REVEALS THE PRESENCE OF A HUMAN T CELL CONTROL REGION (hTCCR) IN PRIMARY T CELLS

While the Jurkat cell line has been widely used to study the transcriptional regulation of *TNFSF11* in T cells [Gendron et al., 2005], the relationship between this cell line and primary human T cells at the *TNFSF11* locus is not entirely clear. Accordingly, we analyzed this region in primary human T cells, TPB T cells as well as naïve and memory T cell populations for analogous histone acetylation marks. TPB T cells were treated with or without antibodies to CD3/LFA-1 for 4 h, and both naïve and memory T cell populations were then subjected to ChIP-chip analysis using antibodies to H4ac and H3K9ac. The results are seen in Figure 3 which document the data tracks representing the $\log_2$ ratio of fluorescence obtained from untreated TPB T cells (track 1), TPB T cells treated with antibodies to CD3/LFA-1 (track 2), naïve T cell (track 3), and memory T cell (track 4) precipitated with antibody to either H4ac (Fig. 3a) or H3K9ac (Fig. 3b). Modestly elevated levels of H4ac and H3K9ac were observed at the hTCCR in the primary human T cell populations as well as in naïve T cells, although the H3K9ac mark was not evident in either naïve or memory T cells (Fig. 3b). Similar marks were also observed in clonally expanded NKT cells at the *TNFSF11* locus (data not shown). RNA pol II occupancy was also examined at the human *TNFSF11* locus in total peripheral blood T cells. However, signals for the presence of this enzyme were not detected. We conclude that similarities in the presence of histone acetylation at both the hTCCR and RLD5a/b regions of the *TNFSF11*

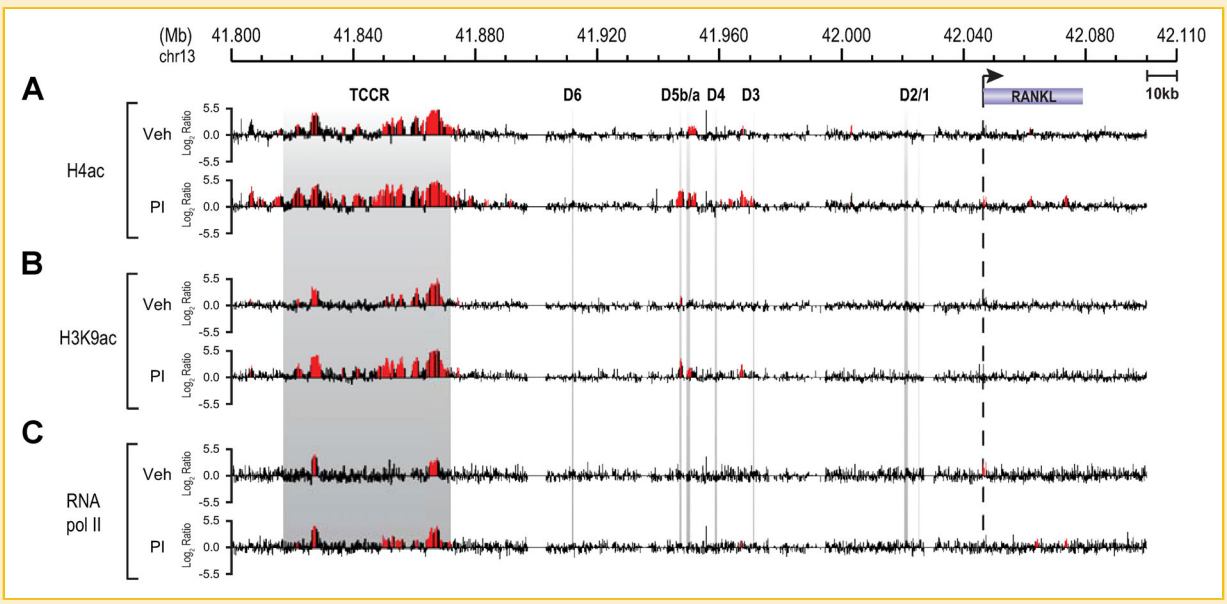

Fig. 2. ChIP-chip analysis identifies the human T cell control region (hTCCR) in Jurkat cells. Jurkat cells were activated with 500 ng/ml ionomycin and 10 ng/ml PMA or vehicle for 6 h and subjected to ChIP-chip analysis using antibodies to tetra-acetylated histone H4 (K5, K8, K12,K16), acetylated histone H3 (K9), and RNA pol II. Immunoprecipitated DNA was amplified by ligation-mediated PCR, labeled with Cy3 or Cy5, and co-hybridized to custom DNA microarrays as described in Materials and Methods. The upper panel depicts the *TNFSF11* gene locus. Nucleotide positions (Mb) are shown on chromosome 13 (March 2006 assembly) while the *TNFSF11* gene and the positions of the distal enhancer regions are indicated below the chromosomal position and designated by descending bands. (A,B,C) Levels of H4ac (A), H3K9ac (B), and RNA pol II (C) at the *TNFSF11* gene locus under vehicle- or PMA/ionomycin-treated conditions. The data tracks represent the $\log_2$ ratios of fluorescence obtained from vehicle or PMA/ionomycin treated samples precipitated with an antibody to H4ac, H3K9ac, RNA pol II, and co-hybridized with labeled ChIP input DNA. All regions highlighted in red represent statistically significant peaks (FDR, $P < 0.05$).

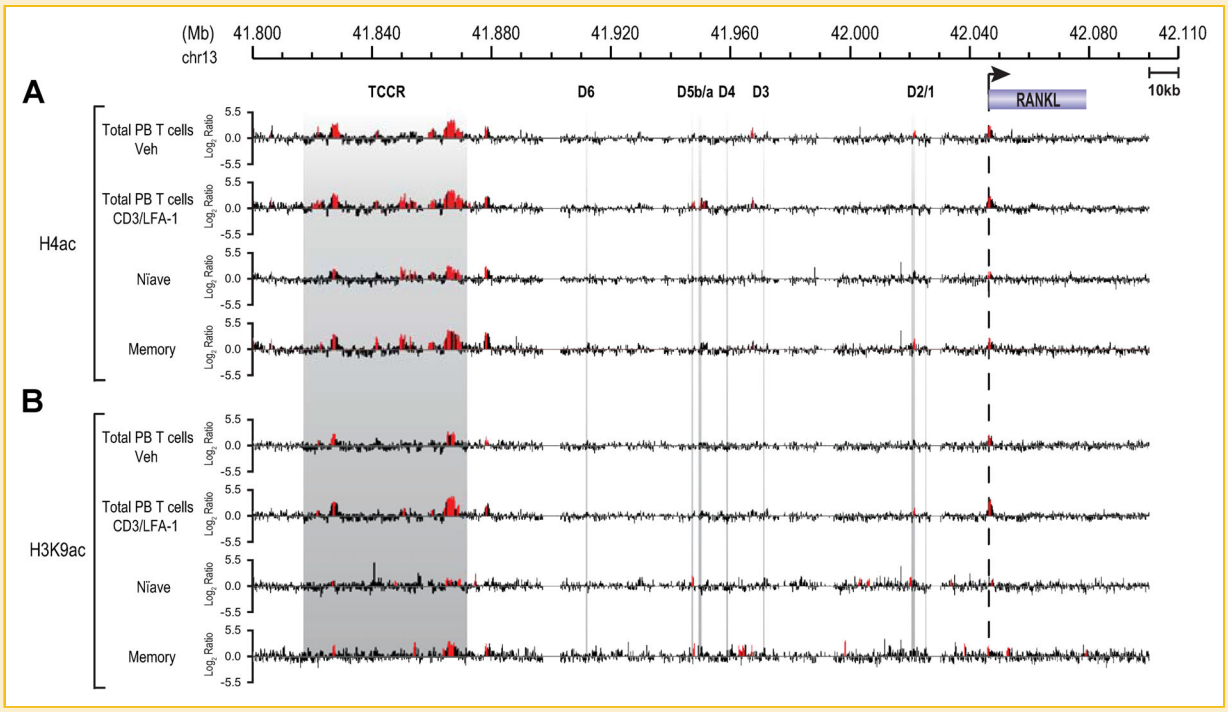

Fig. 3. ChIP-chip analysis confirms that the TCCR is present in primary human T cells prior to activation. Human peripheral blood T cells were treated with or without antibodies to CD3/LFA-1 for 4 h. In addition, naïve and memory T cells were isolated, and all T cell populations were subjected to ChIP-chip analysis using antibodies to tetra-acetylated histone H4 (K5, K8, K12,K16) and acetylated histone H3 (K9). Immunoprecipitated DNA was amplified by ligation-mediated PCR, labeled with Cy3 or Cy5, and co-hybridized to custom DNA microarrays as described in Materials and Methods. The upper panel depicts the *TNFSF11* gene locus. Nucleotide positions (Mb) are shown on chromosome 13 (March 2006 assembly) while the *TNFSF11* gene and the positions of the distal enhancer regions are indicated below the chromosomal position and designated by descending bands. (A,B) Levels of H4ac (A) and H3K9ac (B) enrichment at the *TNFSF11* gene locus. The data tracks represent the $\log_2$ ratios of fluorescence obtained from vehicle (track 1), activated T cells (track 2), naïve T cells (track 3), and memory T cells (track 4) precipitated with an antibody to H4ac or H3K9ac and co-hybridized with a labeled ChIP input DNA. All regions highlighted in red represent statistically significant peaks (FDR, $P < 0.05$).

locus support a potential functional conservation that is reflected in a similarity of regulation of RANKL gene expression between mouse and humans.

MEK1/2 ACTIVATION AND c-FOS RECRUITMENT MODULATE RANKL GENE EXPRESSION

Our recent studies have shown that MEK1/2 activation and AP-1 recruitment are important events associated with transcriptional regulation of the *Tnfsf11* gene in mouse [Bishop et al., 2011]. To provide further support for this signaling pathway in *TNFSF11* activation, we next examined the effects of the MEK1/2 inhibitor U0126 on RANKL expression in Jurkat cells. As can be seen in Figure 4a, a 30-min pretreatment of Jurkat cells with U0126 followed by a 4 h treatment with PI resulted in a dose-dependent inhibition of RANKL mRNA induction. As seen in Figure 4b, the inhibitor also significantly blocked PI-induced upregulation of IL-2 transcripts as well, suggesting that both genes might be regulated by similar transcription factors including c-Fos [Wagner and Eferl, 2005; Kim et al., 2006a; Crispin and Tsokos, 2009]. As this factor had also been observed at the mouse *Tnfsf11* gene locus following T-cell activation [Bishop et al., 2011], we explored the possibility that c-FOS was also involved in regulation of human RANKL expression using ChIP-chip analysis. Jurkat cells were treated with either vehicle or PI and then subjected to ChIP-chip analysis using an antibody to c-Fos. Isolated human peripheral blood T cells, on the other hand, were left either unactivated or activated by antibodies to CD3/LFA-1 and then subjected to ChIP-chip analysis using the same antibody. Figure 4c depicts the data tracks representing the $\log_2$ ratio of fluorescence obtained from Jurkat cells treated with vehicle or PI (tracks 1, 2) and peripheral blood T cells treated with or without antibodies to CD3/LFA-1 (tracks 3, 4) and co-hybridized with corresponding input DNA. As is evident, statistically significant levels of c-FOS were induced primarily across the hTCCR region, but not at the hRLD5a/b region or at the *TNFSF11* promoter. c-FOS binding at the hTCCR in activated primary T cells was not apparent. In total, these results suggest that c-FOS may play an important role in controlling activated RANKL expression in T cells.

THE hTCCR IS CAPABLE OF MEDIATING T CELL ACTIVATION-INDUCED RANKL EXPRESSION

The foregoing ChIP-chip analysis identified the hTCCR as a broad chromatin domain upstream of the *TNFSF11* gene that contains histone modifications and transcription factor recruitment suggestive of enhancer activity. As seen in Figure 5a, an analysis using the 17-way vertebrate alignment tool from the UCSC Genome Browser [Blanchette et al., 2004] revealed that the regions within the hTCCR that contained elevated levels of histone acetylation, RNA pol II occupancy and c-FOS recruitment overlap at least four highly

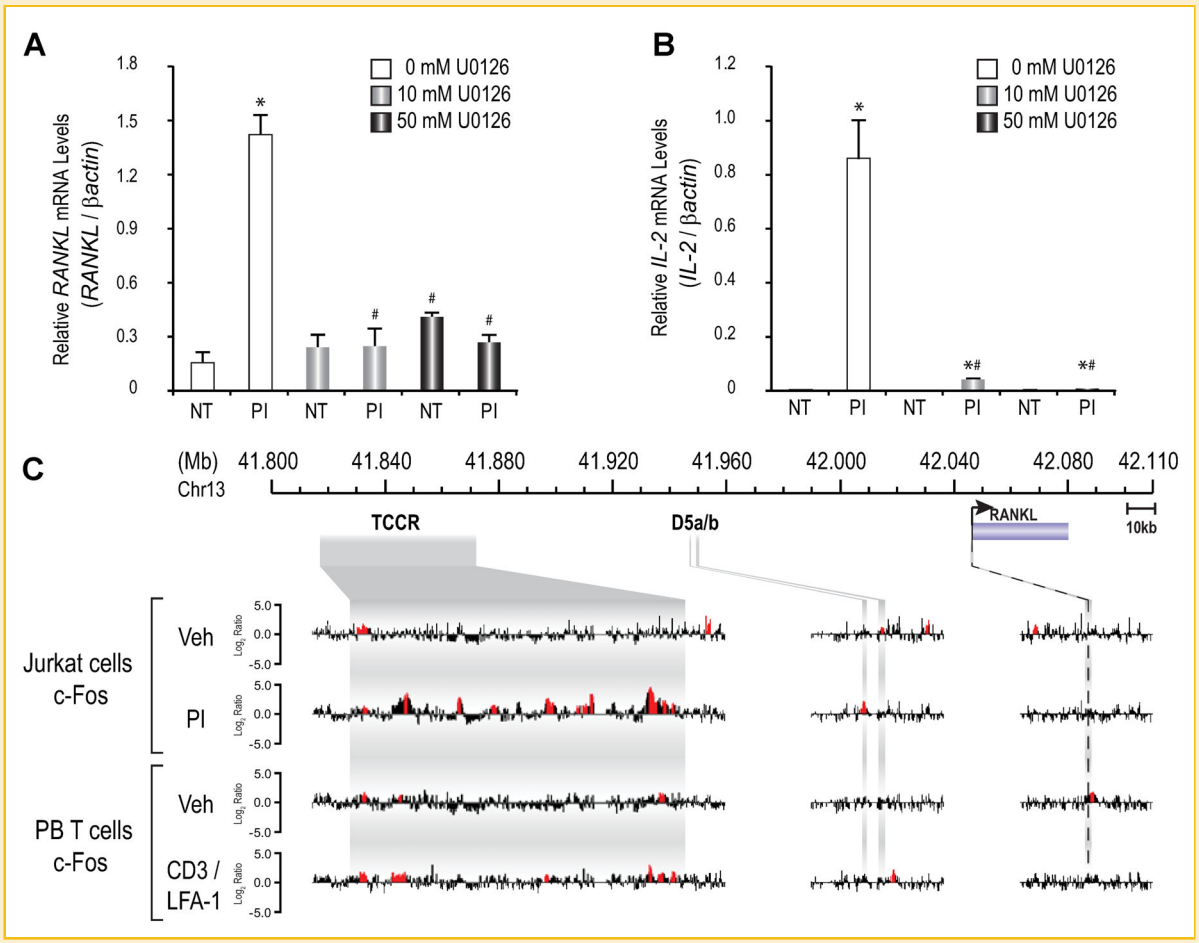

Fig. 4. MEK1/2 activation is necessary for T cell activation-induced *Rankl* gene expression and c-Fos recruitment to the *TNFSF11* locus. (A,B) U0126 treatment inhibited induction of Rankl transcript levels with T-cell activation. Jurkat cells were pretreated with U0126, or vehicle and stimulated with 500 ng/ml ionomycin and 10 ng/ml PMA or vehicle for 4 h. Total RNA was isolated, reverse transcribed, and analyzed by qPCR using primers specific to *Rankl*, *IL-2*, and β-actin. *Rankl* (A) and IL-2 (B) transcript levels were normalized to β-actin. Each value represents the average of three independent experiments ± SEM. $*P < 0.05$, is statistically significant using a non-parametric *t*-test when compared to vehicle-treated sample. $\#P < 0.05$, is statistically significant using a non-parametric *t*-test when compared to 10 μM U0126-treated samples. (C) ChIP-chip analysis identifies both c-Fos recruitment to the human *TNFSF11* locus. Jurkat cells were treated with 500 ng/ml ionomycin and 10 ng/ml PMA or vehicle for 1 h and peripheral blood T cells were treated with or without antibodies to CD3/LFA-1 and subjected to ChIP-chip analysis using an antibodies to c-Fos. Samples were prepared as described in Materials and Methods. The data tracks represent the $\log_2$ ratios of fluorescence obtained from vehicle-treated (track 1, 3) and activated samples (track 2, 4) precipitated with antibodies to c-Fos. All peaks highlighted in red represent statistically significant peaks (FDR, $P < 0.05$).

conserved regions across the locus that we have termed hRLT1A, -T1B, -T2, and -T3, using similar nomenclature established for the mouse TCCR [Bishop et al., 2011]. To examine the activity of these four distinct regions, we cloned a segment of each into a reporter plasmid upstream of the heterologous thymidine kinase (TK) promoter, transfected these constructs into Jurkat cells, and then treated the transfectants for 24 h with either vehicle or PI. As can be seen in Figure 5b, activation by PI induced significant normalized reporter activity in the constructs containing hRLT1A and hRLT2 but not hRLT1B or hRLT3. PI also activated the reporter plasmid that contained the cloned enhancer segment hRLD5, but not those containing any of the other putative enhancers that were identified in the *TNFSF11* locus in osteoblastic cells (Figure 5c). Interestingly, conserved AP1 and NFAT binding elements necessary for inducible mouse mRLT1A reporter were also found within the human hRLT1A reporter construct. Thus, although they were not examined here, it is possible that they too may regulate the transcriptional activity of the hRLT1A region in the hTCCR [Bishop et al., 2011]. Despite this, we conclude that specific regulatory regions within the hTCCR, which are not highlighted through histone marks in osteoblast lineage cells, are likely to regulate *TNFSF11* expression in a unique manner in T cells. Whether these regulatory regions also mediate *TNFSF11* expression in hematopoietic B cells is not known.

BONE MINERAL DENSITY (BMD) ASSOCIATED SNPS ARE PRESENT WITHIN THE hTCCR

Although RANKL is known to play a major role in bone metabolism, its role following expression in T cells has not been established. Nevertheless, several SNPs associated with changes in BMD are located upstream of the *TNFSF11* transcription unit [Styrkarsdottir et al., 2008; Rivadeneira et al., 2009; Styrkarsdottir et al., 2009; Roshandel et al., 2010]. We therefore examined the locations of

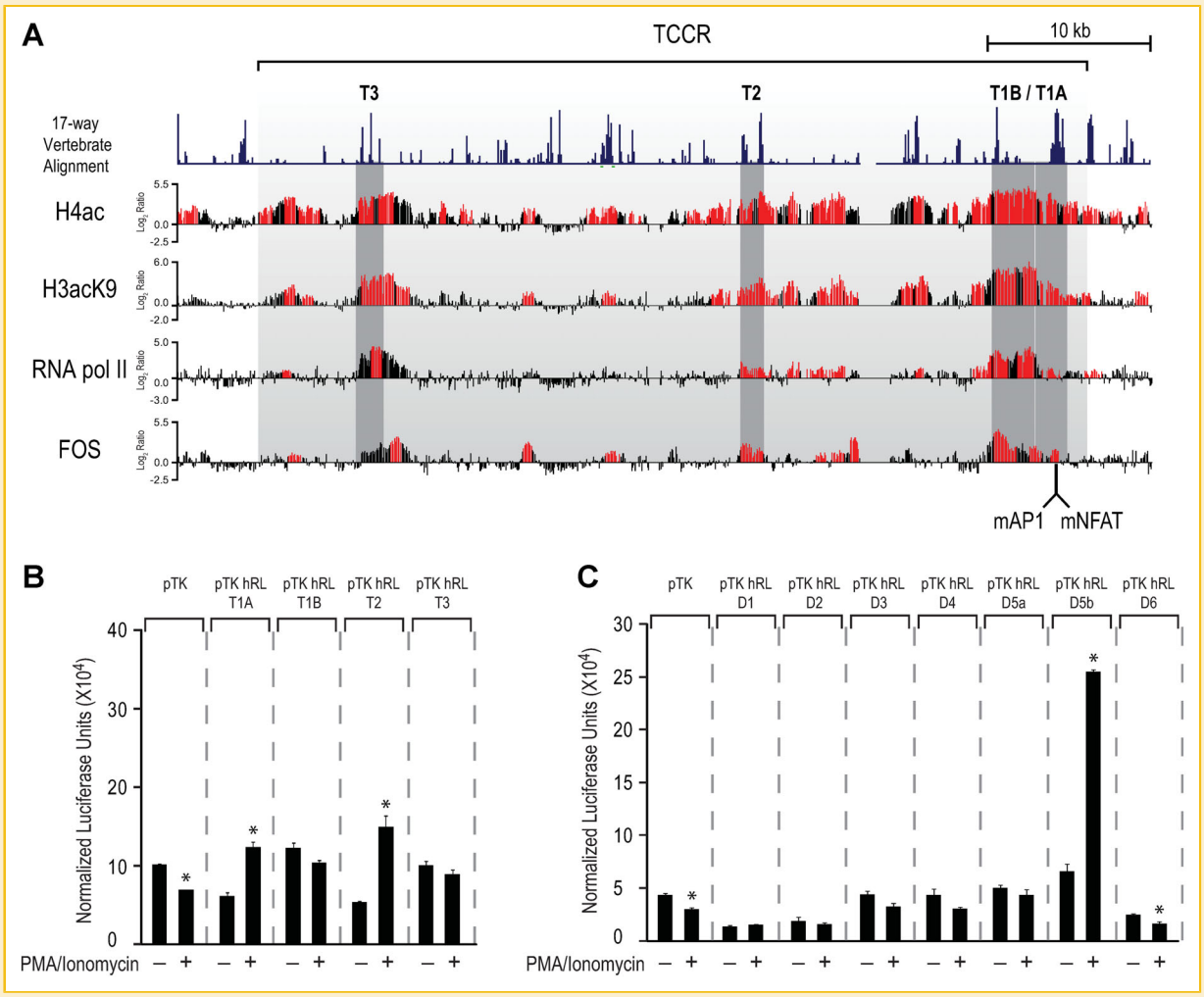

Fig. 5. hTCCR contains highly conserved sequences with transcriptional regulatory capability. (A) The UCSC Genome Browser's 17-way vertebrate alignment (track 1) at Chr13: 41.815–41.875 MB was paired with the ChIP-chip analysis of H4ac (track 2), H4K9ac (track 3), RNA pol II (track 4), and FOS (track 5) recruitment at the human TCCR in PMA/Ionomycin treated Jurkat cells from Figures 2 and 4. Regions containing high sequence conservation and elevated signal in all four ChIP-chip analyses are highlighted in grey (hRL-T1A, T1B, T2, T3) and were cloned into the pTK-luciferase vector. (B,C) hRL-D5b and TCCR regulate reporter activity upon T cell activation. Previously identified TCCR reporter constructs (B) and *TNFSF11* enhancer reporter constructs (C) were co-transfected with pRSV-βgal and treated for 20 h with 500 ng/ml ionomycin and 10 ng/ml PMA or vehicle. Luciferase activity was normalized to β-galactosidase activity. Each value represents the average of three independent experiments ± SEM. *$P < 0.05$ is statistically significant using a non-parametric *t*-test when compared to vehicle-treated sample.

several of these SNPs relative to both the previously identified osteoblast-specific enhancers as well as the T cell specific enhancers identified in this study. As can be seen in Figure 6, rs9594738 [Styrkarsdottir et al., 2008] and rs9533090 [Rivadeneira et al., 2009], SNPs that both reached genome wide significance for BMD in genome-wide association studies, were found to be located within the hTCCR and immediately upstream of hRLD5a/b. Interestingly, rs9594738 was more specifically found to be located within our transcriptionally responsive hRLT2 reporter construct. We hypothesize that this particular single base pair change might affect enhancer activity through modulation of transcription factor binding activity [Guttormsen et al., 2008; Tuupanen et al., 2009; Wright et al., 2010]. In silico analysis predicted a change in affinity for several transcription factors within this rs9594738 (C/T) allele, although we have yet to identify a specific factor that might be involved in modulating the activity of this hRLT2 enhancer.

DISCUSSION

Over the past decade, the RANKL-RANK-Osteoprotegerin signaling axis has been shown to play an important role in regulating the proliferation, differentiation, and survival of various cell types throughout the body [Anderson et al., 1997; Wong et al., 1997b; Fata et al., 2000; Loser et al., 2006; Leibbrandt and Penninger, 2008]. While T cell production of RANKL is thought to be involved in the survival of dendritic cells [Anderson et al., 1997; Wong et al., 1997a,b] and potentially inflammation and autoimmune

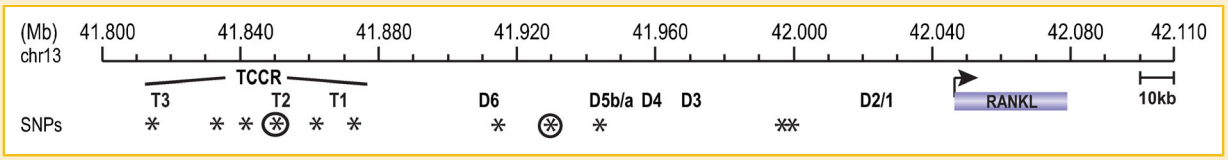

Fig. 6. SNPs associated with BMD are located within the enhancers identified in the *TNFSF11* gene locus. The *TNFSF11* gene locus is shown at the top of the figure together with nucleotide positions on chromosome 13 (Hg18). The locations of the *TNFSF11* enhancers identified in earlier studies as well as those present in the current study are identified. Asterisks (*) denote the locations of SNPs that are associated with BMD in genome-wide studies. Asterisks that are circled reach genome-wide significance in genome wide association studies [Styrkarsdottir et al., 2008, 2009; Rivadeneira et al., 2009; Roshandel et al., 2010].

related bone breakdown, recent studies have also highlighted the utility of B cells in controlling bone metabolism during chronic inflammation. Still, little is known about the mechanisms involved in the production and regulation of the *TNFSF11* gene in human lymphoid cells. The work presented here details some of the molecular events involved in the transcription of the human *TNFSF11* gene upon T cell activation.

Our studies show that RANKL is indeed upregulated in both a T cell line and in freshly isolated human peripheral blood T lymphocytes as well as in naïve and memory T cells following T cell activation by either PI or by anti-CD3/LFA-1 antibodies. This upregulation was rapid and generally transient. An examination of certain features of the genetic and epigenetic landscape of the *TNFSF11* gene locus in Jurkat cells demonstrated enrichment for H4ac and H3K9ac as well as increased abundance of RNA pol II within two upstream regions of the gene locus, which we have termed the hTCCR, and the hRLD5a/b. While the latter appears functional at the *TNFSF11* gene locus in osteoblast lineage cells, the former appears to be unique to T cells. These observations reflect similar findings at the mouse *Tnfsf11* gene locus. A subset of these *TNFSF11* gene features were found in primary T cells as well. Additional studies suggest that T cell activation, particularly in the Jurkat T cell model, results in stimulation and MEK1/2 activated induction of c-Fos recruitment to various sub-elements within the hTCCR. The independent insertion of these regions into a reporter construct followed by transfection in Jurkat T cells demonstrated that the activity of at least two of the four identified enhancers within the hTCCR could be directly upregulated through PI activation. We conclude from these studies that both the mouse and human *TNFSF11* genes retain highly conserved structural and functional features at their individual loci, and that like the mouse gene, the human *TNFSF11* gene regulatory locus is comprised of a series of osteoblast lineage active regulatory enhancers and a series of T cell activate regulatory enhancers as well.

Our approach in characterizing the regulatory features of the human *TNFSF11* gene was similar to that which we applied early on to our study of the mouse *Tnfsf11* gene: to utilize unbiased ChIP-chip analysis to identify specific regions across extended loci to which important regulatory factors might be induced to occupy or that retain epigenetic marks or activity features that are reflective of potential enhancers [Bishop et al., 2009; Meyer et al., 2010; Zella et al., 2010]. These regions were then scrutinized further using more traditional methods. This approach identified a highly remote region upstream of the mouse *Tnfsf11* TSS that mediated upregulation of Rankl expression in mouse T cells and has now been used to identify an analogous structural and functional region in the human gene [Bishop et al., 2011]. Interestingly, while both genes are similar in organization, they are not identical. Thus, while the mRLD5 region is the primary mediator of $1,25(OH)_2D_3$ response in the mouse gene, a more proximal element termed hRLD2 located at −20 kb is likely responsible for this activity in human cells [Nerenz et al., 2008]. In the past few years, the method of ChIP-chip analysis has rapidly been replaced by ChIP-seq analysis, largely due to sensitivity and accuracy. Nevertheless, in the subset of studies where ChIP-seq has been applied including our own, the results observed have confirmed those identified using the earlier ChIP-chip technology [Pike and Meyer, 2014; Pike et al., 2014; Meyer et al., 2014a].

The results obtained in this study suggest that two distinct collections of enhancers are likely responsible for *TNFSF11* gene expression, one that regulates transcriptional output in osteoblast lineage cells and the other in T cells. We also note that these enhancer regions are located many kilobases upstream of the *TNFSF11* gene promoter as are those that regulate the mouse *Tnfsf11* gene as well. While this was thought to be an unusual feature of this particular gene early on, it is now clear that multiple elements located highly distal to the gene itself may represent the norm rather than the exception [Meyer et al., 2014a,b]. This structural organization implies highly complex and cell-specific regulated DNA looping that must serve to juxtapose the multiple regulatory elements near the *TNFSF11* gene promoter in a cell-type specific manner. Importantly, we identified the presence of such a looping structure in the mouse *Tnfsf11* gene [Bishop et al., 2011]. The signaling pathways that activate these two distinct collections are clearly different. Interestingly, however, it appears that some overlap may also be present, as the RLD5a/b region contributes activity both in osteoblasts and in immune cells. Indeed, while this concept originated in studies conducted largely in cells in vitro [Fu et al., 2006; Kim et al., 2006b], they are also supported by a detailed study conducted in vivo wherein the RLD5a/b enhancer was deleted from the mouse genome and shown to cause a reduction in RANKL expression in both skeletal cells and immune tissues such as spleen and thymus [Galli et al., 2008]. An analysis of the skeletal and immune consequences of genomic deletion of several additional mouse *Tnfsf11* enhancers in vivo is currently in progress including one associated with the TCCR. Based upon these observations, while the capacity of distinct enhancers to regulate expression of genes in a cell-specific manner is a recurring theme in biology it appears that the *TNFSF11* gene is no exception.

A recent report suggests that significant overexpression of RANKL from a human bacterial artificial chromosome (BAC) clone that contained the human *TNFSF11* gene locus was capable in a transgenic

copy-dependent and RANKL concentration-dependent manner of inducing severe early onset bone loss [Rinotas et al., 2014]. This feature was characterized in the extreme by lack of trabecular bone, destruction of the growth plate, increased osteoclastogenesis, bone marrow adiposity, increased bone remodeling, and severe cortical bone porosity accompanied by decreased bone strength. BAC-derived RANKL was broadly expressed as a function of the strains in a wide variety of tissues, although it was not evident from this tissue distribution that the BAC transgene was in fact producing RANKL in a tissue-selective manner similar to that of the endogenous gene or that this expression was due to the regulatory features associated with the endogenous *TNFSF11* gene locus. Introduction of this transgene into a mouse containing a loss of function *Tnfsf11* allele that phenocopied Rankl-deficient mice rescued in copy-dependent fashion many of the features of this altered mouse, leading the authors to suggest that this human transgene was capable of restoring RANKL expression in an appropriate fashion. While the authors acknowledge that the *TNFSF11* gene is regulated by distal enhancers, however, selection of the BAC transgene was not based upon an analysis of the human gene′s regulatory domains but rather was arbitrary, containing only 75.4 kb of DNA sequence upstream of the *TNFSF11* gene′s TSS. Given our previous studies as well as those reported herein, the construct used by these investigators could not contain the key regulatory enhancer RLD5a/b located upstream of 75.4 kb at −95 kb or the hTCCR located between −170 and −220 kb. The absence of these key regulatory elements is almost certain to result in aberrant expression of the *TNFSF11* gene in mouse tissues relative to the expression of the endogenous *Tnfsf11* gene, the absence of Rankl expression in T cells and perhaps other cells of the hematopoietic lineage, and likely is responsible for the tissue distribution of BAC-derived RANKL that was actually observed. Thus, it seems likely that this animal model is simply one of untargeted overexpression of RANKL that when coupled to pre-existing endogenous levels of mouse Rankl resulted in the extensive osteoporotic phenotype that was observed.

In summary, we have identified a broad intergenic region located between −170 and −220 kb upstream of the human *TNFSF11* gene that participates in the regulated expression of the human *TNFSF11* gene in T cells. This region, termed the hTCCR, together with the RLD5a/b enhancer located at −95 kb, are evident when genetic and epigenetic features of the *TNFSF11* gene are examined in both human Jurkat cells and in primary human T cell subsets. We conclude that both the mouse and human *TNFSF11* genes are structurally organized and functionally regulated in a very similar fashion.

ACKNOWLEDGMENTS

We thank members of the Pike Lab for their helpful discussions and contributions to this manuscript. This work was supported by National Institute of Diabetes, Digestive and Kidney Diseases grant DK-074993.

REFERENCES

Anderson DM, Maraskovsky E, Billingsley WL, Dougall WC, Tometsko ME, Roux ER, Teepe MC, DuBose RF, Cosman D, Galibert L. 1997. A homologue of the TNF receptor and its ligand enhance T-cell growth and dendritic-cell function. Nature 390:175–179.

Bishop KA, Coy HM, Nerenz RD, Meyer MB, Pike JW. 2011. Mouse Rankl expression is regulated in T cells by c-Fos through a cluster of distal regulatory enhancers designated the T cell control region. J Biol Chem 286:20880–20891.

Bishop KA, Meyer MB, Pike JW. 2009. A novel distal enhancer mediates cytokine induction of mouse RANKl gene expression. Mol Endocrinol 23:2095–2110.

Blanchette M, Kent WJ, Riemer C, Elnitski L, Smit AF, Roskin KM, Baertsch R, Rosenbloom K, Clawson H, Green ED, Haussler D, Miller W. 2004. Aligning multiple genomic sequences with the threaded blockset aligner. Genome Res 14:708–715.

Burkiewicz JS, Scarpace SL, Bruce SP. 2009. Denosumab in osteoporosis and oncology. Ann Pharmacother 43:1445–1455.

Choi JK, Howe LJ. 2009. Histone acetylation: Truth of consequences? Biochem Cell Biol 87:139–150.

Crispin JC, Tsokos GC. 2009. Transcriptional regulation of IL-2 in health and autoimmunity. Autoimmun Rev 8:190–195.

Dai SM, Nishioka K, Yudoh K. 2004. Interleukin (IL) 18 stimulates osteoclast formation through synovial T cells in rheumatoid arthritis: Comparison with IL1 beta and tumour necrosis factor alpha. Ann Rheum Dis 63:1379–1386.

Ernst J, Kheradpour P, Mikkelsen TS, Shoresh N, Ward LD, Epstein CB, Zhang X, Wang L, Issner R, Coyne M, Ku M, Durham T, Kellis M, Bernstein BE. 2011. Mapping and analysis of chromatin state dynamics in nine human cell types. Nature 473:43–49.

Fata JE, Kong YY, Li J, Sasaki T, Irie-Sasaki J, Moorehead RA, Elliott R, Scully S, Voura EB, Lacey DL, Boyle WJ, Khokha R, Penninger JM. 2000. The osteoclast differentiation factor osteoprotegerin-ligand is essential for mammary gland development. Cell 103:41–50.

Fionda C, Nappi F, Piccoli M, Frati L, Santoni A, Cippitelli M. 2007. 15-deoxy-Delta12,14-prostaglandin J2 negatively regulates rankl gene expression in activated T lymphocytes: Role of NF-kappaB and early growth response transcription factors. J Immunol 178:4039–4050.

Fu Q, Manolagas SC, O′Brien CA. 2006. Parathyroid hormone controls receptor activator of NF-kappaB ligand gene expression via a distant transcriptional enhancer. Mol Cell Biol 26:6453–6468.

Galli C, Zella LA, Fretz JA, Fu Q, Pike JW, Weinstein RS, Manolagas SC, O′Brien CA. 2008. Targeted deletion of a distant transcriptional enhancer of the receptor activator of nuclear factor-kappaB ligand gene reduces bone remodeling and increases bone mass. Endocrinology 149:146–153.

Gendron S, Couture J, Aoudjit F. 2005. Collagen type I signaling reduces the expression and the function of human receptor activator of nuclear factor-kappa B ligand (RANKL) in T lymphocytes. Eur J Immunol 35:3673–3682.

Guttormsen J, Koster MI, Stevens JR, Roop DR, Williams T, Winger QA. 2008. Disruption of epidermal specific gene expression and delayed skin development in AP-2 gamma mutant mice. Dev Biol 317:187–195.

Jimi E, Akiyama S, Tsurukai T, Okahashi N, Kobayashi K, Udagawa N, Nishihara T, Takahashi N, Suda T. 1999. Osteoclast differentiation factor acts as a multifunctional regulator in murine osteoclast differentiation and function. J Immunol 163:434–442.

Josien R, Wong BR, Li HL, Steinman RM, Choi Y. 1999. TRANCE, a TNF family member, is differentially expressed on T cell subsets and induces cytokine production in dendritic cells. J Immunol 162:2562–2568.

Kanamaru F, Iwai H, Ikeda T, Nakajima A, Ishikawa I, Azuma M. 2004. Expression of membrane-bound and soluble receptor activator of NF-kappaB ligand (RANKL) in human T cells. Immunol Lett 94:239–246.

Kim HP, Imbert J, Leonard WJ. 2006a. Both integrated and differential regulation of components of the IL-2/IL-2 receptor system. Cytokine Growth Factor Rev 17:349–366.

Kim S, Shevde NK, Pike JW. 2005. 1,25-Dihydroxyvitamin D_3 stimulates cyclic vitamin D receptor/retinoid X receptor DNA-binding, co-activator

recruitment, and histone acetylation in intact osteoblasts. J Bone Miner Res 20:305–317.

Kim S, Yamazaki M, Shevde NK, Pike JW. 2007. Transcriptional control of receptor activator of nuclear factor-kappaB ligand by the protein kinase A activator forskolin and the transmembrane glycoprotein 130-activating cytokine, oncostatin M, is exerted through multiple distal enhancers. Mol Endocrinol 21:197–214.

Kim S, Yamazaki M, Zella LA, Shevde NK, Pike JW. 2006b. Activation of receptor activator of NF-kappaB ligand gene expression by 1,25-dihydroxyvitamin D_3 is mediated through multiple long-range enhancers. Mol Cell Biol 26:6469–6486.

Kurdistani SK, Tavazoie S, Grunstein M. 2004. Mapping global histone acetylation patterns to gene expression. Cell 117:721–733.

Lacey DL, Timms E, Tan HL, Kelley MJ, Dunstan CR, Burgess T, Elliott R, Colombero A, Elliott G, Scully S, Hsu H, Sullivan J, Hawkins N, Davy E, Capparelli C, Eli A, Qian YX, Kaufman S, Sarosi I, Shalhoub V, Senaldi G, Guo J, Delaney J, Boyle WJ. 1998. Osteoprotegerin ligand is a cytokine that regulates osteoclast differentiation and activation. Cell 93:165–176.

Leibbrandt A, Penninger JM. 2008. RANK/RANKL: Regulators of immune responses and bone physiology. Ann N Y Acad Sci 1143:123–150.

Loser K, Mehling A, Loeser S, Apelt J, Kuhn A, Grabbe S, Schwarz T, Penninger JM, Beissert S. 2006. Epidermal RANKL controls regulatory T-cell numbers via activation of dendritic cells. Nat Med 12:1372–1379.

Meyer MB, Benkusky NA, Lee CH, Pike JW. 2014a. Genomic determinants of gene regulation by 1,25-dihydroxyvitamin D_3 during osteoblast-lineage cell differentiation. J Biol Chem 289:19539–19554.

Meyer MB, Benkusky NA, Pike JW. 2014b. The RUNX2 cistrome in osteoblasts: Characterization, down-regulation following differentiation, and relationship to gene expression. J Biol Chem 289:16016–16031.

Meyer MB, Goetsch PD, Pike JW. 2010. A downstream intergenic cluster of regulatory enhancers contributes to the induction of CYP24A1 expression by 1alpha,25-dihydroxyvitamin D_3. J Biol Chem 285:15599–15610.

Nakashima T, Wada T, Penninger JM. 2003. RANKL and RANK as novel therapeutic targets for arthritis. Curr Opin Rheumatol 15:280–287.

Nerenz RD, Martowicz ML, Pike JW. 2008. An enhancer 20 kilobases upstream of the human receptor activator of nuclear factor-kappaB ligand gene mediates dominant activation by 1,25-dihydroxyvitamin D_3. Mol Endocrinol 22:1044–1056.

Pike JW, Lee SM, Meyer MB. 2014. Regulation of gene expression by 1,25-dihydroxyvitamin D_3 in bone cells: Exploiting new approaches and defining new mechanisms. Bonekey Rep 3:482.

Pike JW, Meyer MB. 2014. Fundamentals of vitamin D hormone-regulated gene expression. J Steroid Biochem Mol Biol 144:5–11.

Rinotas V, Niti A, Dacquin R, Bonnet N, Stolina M, Han CY, Kostenuik P, Jurdic P, Ferrari S, Douni E. 2014. Novel genetic models of osteoporosis by overexpression of human RANKL in transgenic mice. J Bone Miner Res 29:1158–1169.

Rivadeneira F, Styrkarsdottir U, Estrada K, Halldorsson BV, Hsu YH, Richards JB, Zillikens MC, Kavvoura FK, Amin N, Aulchenko YS, Cupples LA, Deloukas P, Demissie S, Grundberg E, Hofman A, Kong A, Karasik D, van Meurs JB, Oostra B, Pastinen T, Pols HA, Sigurdsson G, Soranzo N, Thorleifsson G, Thorsteinsdottir U, Williams FM, Wilson SG, Zhou Y, Ralston SH, van Duijn CM, Spector T, Kiel DP, Stefansson K, Ioannidis JP, Uitterlinden AG. 2009. Twenty bone-mineral-density loci identified by large-scale meta-analysis of genome-wide association studies. Nat Genet 41:1199–1206.

Roh TY, Cuddapah S, Zhao K. 2005. Active chromatin domains are defined by acetylation islands revealed by genome-wide mapping. Genes Dev 19:542–552.

Roh TY, Wei G, Farrell CM, Zhao K. 2007. Genome-wide prediction of conserved and nonconserved enhancers by histone acetylation patterns. Genome Res 17:74–81.

Roshandel D, Holliday K, Pye SR, Boonen S, Borghs H, Vanderschueren D, Huhtaniemi IT, Adams JE, Ward KA, Bartfai G, Casanueva F, Finn JD, Forti G, Giwercman A, Han TS, Kula K, Lean ME, Pendleton N, Punab M, Silman AJ, Wu FC, Thomson W, O'Neill TW. 2010. Genetic variation in the RANKL/RANK/OPG signaling pathway is associated with bone turnover and bone mineral density in men. J Bone Miner Res 25:1830–1838.

Schubeler D, MacAlpine DM, Scalzo D, Wirbelauer C, Kooperberg C, van Leeuwen F, Gottschling DE, O'Neill LP, Turner BM, Delrow J, Bell SP, Groudine M. 2004. The histone modification pattern of active genes revealed through genome-wide chromatin analysis of a higher eukaryote. Genes Dev 18:1263–1271.

Silverman SL. 2009. New therapies for osteoporosis: Zoledronic acid, bazedoxifene, and denosumab. Curr Osteoporos Rep 7:91–95.

Styrkarsdottir U, Halldorsson BV, Gretarsdottir S, Gudbjartsson DF, Walters GB, Ingvarsson T, Jonsdottir T, Saemundsdottir J, Center JR, Nguyen TV, Bagger Y, Gulcher JR, Eisman JA, Christiansen C, Sigurdsson G, Kong A, Thorsteinsdottir U, Stefansson K. 2008. Multiple genetic loci for bone mineral density and fractures. N Engl J Med 358:2355–2365.

Styrkarsdottir U, Halldorsson BV, Gretarsdottir S, Gudbjartsson DF, Walters GB, Ingvarsson T, Jonsdottir T, Saemundsdottir J, Snorradottir S, Center JR, Nguyen TV, Alexandersen P, Gulcher JR, Eisman JA, Christiansen C, Sigurdsson G, Kong A, Thorsteinsdottir U, Stefansson K. 2009. New sequence variants associated with bone mineral density. Nat Genet 41:15–17.

Suda T, Takahashi N, Martin TJ. 1992. Modulation of osteoclast differentiation. Endocr Rev 13:66–80.

Teitelbaum SL. 2000. Bone resorption by osteoclasts. Science 289:1504–1508.

Tuupanen S, Turunen M, Lehtonen R, Hallikas O, Vanharanta S, Kivioja T, Bjorklund M, Wei G, Yan J, Niittymaki I, Mecklin JP, Jarvinen H, Ristimaki A, Di-Bernardo M, East P, Carvajal-Carmona L, Houlston RS, Tomlinson I, Palin K, Ukkonen E, Karhu A, Taipale J, Aaltonen LA. 2009. The common colorectal cancer predisposition SNP rs6983267 at chromosome 8q24 confers potential to enhanced Wnt signaling. Nat Genet 41:885–890.

Wagner EF, Eferl R. 2005. Fos/AP-1 proteins in bone and the immune system. Immunol Rev 208:126–140.

Wang Z, Zang C, Rosenfeld JA, Schones DE, Barski A, Cuddapah S, Cui K, Roh TY, Peng W, Zhang MQ, Zhao K. 2008. Combinatorial patterns of histone acetylations and methylations in the human genome. Nat Genet 40:897–903.

Wang R, Zhang L, Zhang X, Moreno J, Celluzzi C, Tondravi M, Shi Y. 2002. Regulation of activation-induced receptor activator of NF-kappaB ligand (RANKL) expression in T cells. Eur J Immunol 32:1090–1098.

Wong BR, Josien R, Lee SY, Sauter B, Li HL, Steinman RM, Choi Y. 1997a. TRANCE (tumor necrosis factor [TNF]-related activation-induced cytokine), a new TNF family member predominantly expressed in T cells, is a dendritic cell-specific survival factor. J Exp Med 186:2075–2080.

Wong BR, Rho J, Arron J, Robinson E, Orlinick J, Chao M, Kalachikov S, Cayani E, Bartlett FS, 3rd, Frankel WN, Lee SY, Choi Y. 1997b. TRANCE is a novel ligand of the tumor necrosis factor receptor family that activates c-Jun N-terminal kinase in T cells. J Biol Chem 272:25190–25194.

Wright JB, Brown SJ, Cole MD. 2010. Upregulation of c-MYC in cis through a large chromatin loop linked to a cancer risk-associated single-nucleotide polymorphism in colorectal cancer cells. Mol Cell Biol 30:1411–1420.

Yamamoto H, Shevde NK, Warrier A, Plum LA, DeLuca HF, Pike JW. 2003. 2-Methylene-19-nor-(20S)-1,25-dihydroxyvitamin D3 potently stimulates gene-specific DNA binding of the vitamin D receptor in osteoblasts. J Biol Chem 278:31756–31765.

Zella LA, Meyer MB, Nerenz RD, Lee SM, Martowicz ML, Pike JW. 2010. Multifunctional enhancers regulate mouse and human vitamin D receptor gene transcription. Mol Endocrinol 24:128–147.